HERSCHEL / PLANCK

CDR HERSCHEL Micro-Vibration Analysis Report H-P-2-ASP-AN-0773

	Responsabilité-Service-Société *Responsibility-Office –Company*	Date	Signature
Rédigé par/*Written by*	System Mechanical Analyses team		
Vérifié par/*Verified by*	System Mechanical Analyses P. LODEREAU	9/07/04	
Approbation/*Approved*	Sciences/Obs. Satellite Group Manager R. VIALE	9/07/04	
Approbation/*Approved*	System Mechanical Architecture Ph. CLAVEL	20/07/04	
Approbation/*Approved*	System Engineering Manager P.RIDEAU	20/07/04	
Approbation/*Approved*	PA Manager C. MASSE	20/07/04	
Approbation/*Approved*	Project Manager J.J. JUILLET	20/07/04	

Entité Emettrice : Alcatel Space - Cannes
(détentrice de l'original) :

HERSCHEL/PLANCK	DISTRIBUTION RECORD

DOCUMENT NUMBER : H-P-2-ASP-AN-0773

Issue 1/ Rev. : 0
Date: 25/06/2004

EXTERNAL DISTRIBUTION		INTERNAL DISTRIBUTION	
ESA	X	HP team	X
ASTRIUM			
ALENIA			
CONTRAVES			
TICRA			
TECNOLOGICA			
		Clt Documentation	Orig.

ENREGISTREMENT DES EVOLUTIONS / CHANGE RECORDS

ISSUE	DATE	§ : DESCRIPTION DES EVOLUTIONS § : CHANGE RECORD	REDACTEUR AUTHOR

TABLE OF CONTENTS

LIST OF TABLES

LIST OF FIGURES

1 APPLICABLE & REFERENCE DOCUMENTS

[RD1] ACMS Glossary_update
H-P-4-DS-TN-017_2_0

[RD2] CDR Herschel Dynamic Analysis and Sine Test Prediction Report
H-P-2-ASPI-AN-0719, Issue 1.0

[RD3] Duch Space /SENER ACMS
H-P-4 ANA-TN-006, Issue 3.0

[RD4] RFD Duch space
HP-TX-RFD-0003 rev 1 dated 02/12/03

[RD5] Herschel /Planck Instrument Interface Document part B instrument "SPIRE"
SCI-PT-IIDB/SPIRE-02124 Issue 3.2 dated 01/03/04

Software version:

- Nastran 70.
- Microvision 4.2.
- Matlab6.5.

2 INTRODUCTION

Microvibrations are critical for the SPIRE instrument of the Herschel spacecraft. They generate disturbing vibrations on the focal plane equipment.
The main source of perturbation identified are the four reaction wheels used to adjust the orientation of Herschel. They are operating at a rotating speed which may vary between 0 and 45 Hz. The AOCS profile taken into account is given in ref. [3]. The wheels are characterised by their static imbalance that generate a radial force and by an axial force. They are both applied at the centre of Gravity of the wheel. Considering the results from PDR phase and checked by primary CDR analysis, the dynamic imbalance that represents less than 2% of the perturbation has not been taken into account.
The aim of this analysis is to determine the level of acceleration at the centre of gravity of the SPIRE FPU due to the reaction wheels perturbation.

3 HERSCHEL SPACECRAFT

HERSCHEL spacecraft f.e.m. view:

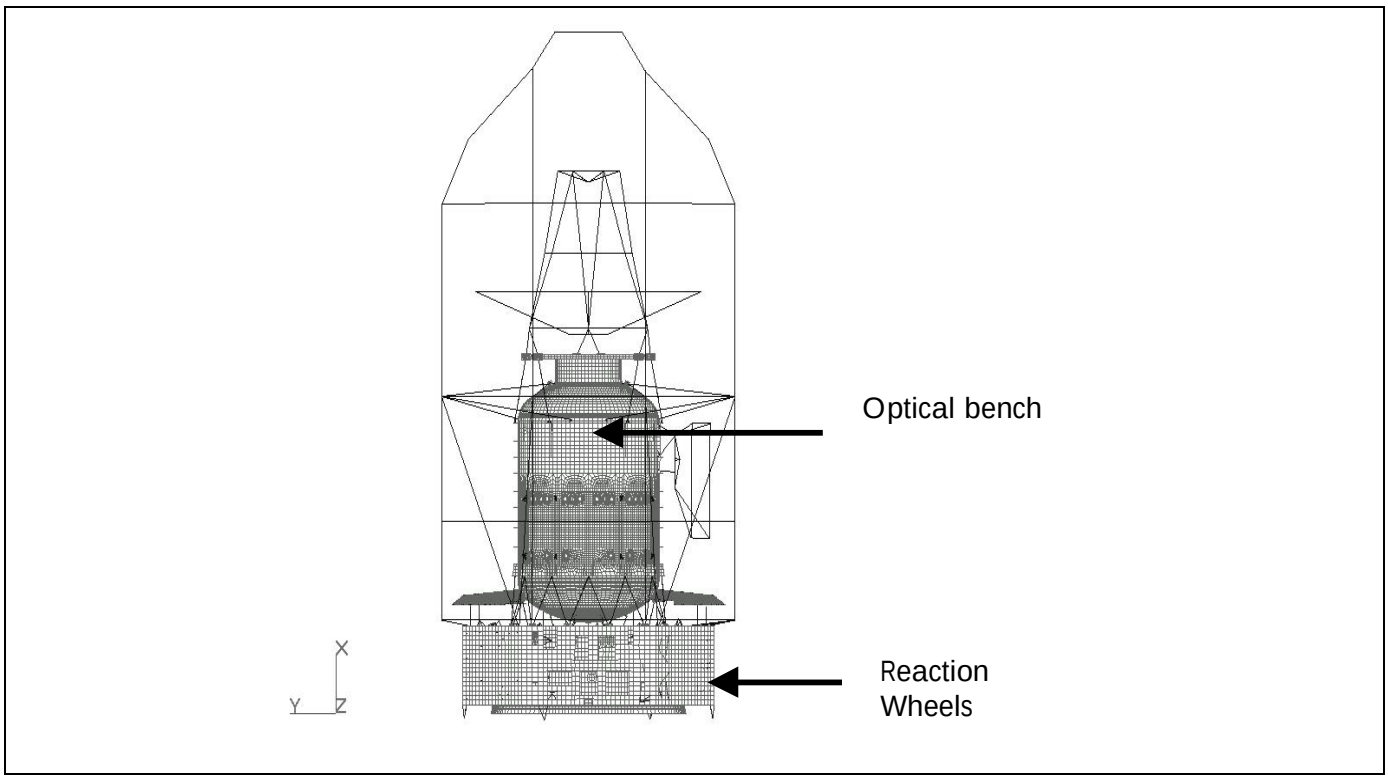

Figure 1:HERSCHEL spacecraft fem view

The structural damping factor has been set to 0.5% to consider a structural damping adapted to microvibration.

The model used for this analysis is described in [RD2].

3.1 MCI

The following table shows spacecraft cog and mass properties.

```
      O U T P U T   F R O M   G R I D   P O I N T   W E I G H T   G E N E R A T O R
                                REFERENCE POINT =       0
                                        M O
   *  3.382553E+03 -3.583693E-10 -1.802785E-09  1.635470E-09 -1.946209E+00 -4.064157E+00 *
   * -3.583693E-10  3.382553E+03  3.695160E-10  1.949139E+00 -1.277222E-09  6.733414E+03 *
   * -1.802785E-09  3.695160E-10  3.382553E+03  4.006843E+00 -6.733414E+03 -4.656568E-10 *
   *  1.635470E-09  1.949139E+00  4.006843E+00  4.468877E+03  1.861800E+02 -5.847768E+02 *
   * -1.946209E+00 -1.277222E-09 -6.733414E+03  1.861800E+02  2.160342E+04  1.404142E+00 *
   * -4.064157E+00  6.733414E+03 -4.656568E-10 -5.847768E+02  1.404142E+00  2.207971E+04 *
                                        S
                     *  1.000000E+00  0.000000E+00  0.000000E+00 *
                     *  0.000000E+00  1.000000E+00  0.000000E+00 *
                     *  0.000000E+00  0.000000E+00  1.000000E+00 *

DIRECTION
MASS AXIS SYSTEM (S)     MASS              X-C.G.        Y-C.G.        Z-C.G.
X                      3.382553E+03      4.835017E-13  1.201506E-03 -5.753667E-04
Y                      3.382553E+03      1.990630E+00 -3.775910E-13 -5.762331E-04
Z                      3.382553E+03      1.990630E+00  1.184562E-03 -1.376643E-13

                                        I(S)
                     *  4.468872E+03 -1.941561E+02  5.886569E+02 *
                     * -1.941561E+02  8.199684E+03 -1.401804E+00 *
                     *  5.886569E+02 -1.401804E+00  8.675973E+03 *
                                        I(Q)
                     *  8.208247E+03                             *
                     *                4.378357E+03               *
                     *                                8.757924E+03 *
                                         Q
                     * -4.361448E-02 -9.894923E-01  1.378507E-01 *
                     * -9.976985E-01  5.030945E-02  4.546009E-02 *
                     * -5.191760E-02 -1.355507E-01 -9.894092E-01 *
```

The spacecraft total mass is 3382 kg. A complete description of the HERSCHEL fem is given in [RD2].

4 REACTION WHEELS

Each reaction wheel is represented by a rigid body connecting together its 4 interface points enabling introduction of interface disturbances (Figure 2).

Wheel number	Node ID	Analysis Coordinate System
1	17188	13003
2	17189	13002
3	17186	13004
4	17187	13001

Table 1

The disturbance is modelled as a radial force and an axial force that are both applied at the centre of Gravity of the wheel (ref. annex 1)
A local rectangular co-ordinate system is attached to each wheel and defined as follows:

- Origin at the centre of gravity of the wheel
- Y direction parallel to the wheel rotation axis
- (X, Z) plane parallel to the wheel mounting plane

The SPIRE optical instrument is represented by a point mass connected to the structure with a rigid body element. It is assumed that there is no mode local to the optical instrument below 350Hz. Outputs of the computations are presented at its CoG. The node corresponding to the optical instrument is node 48301.

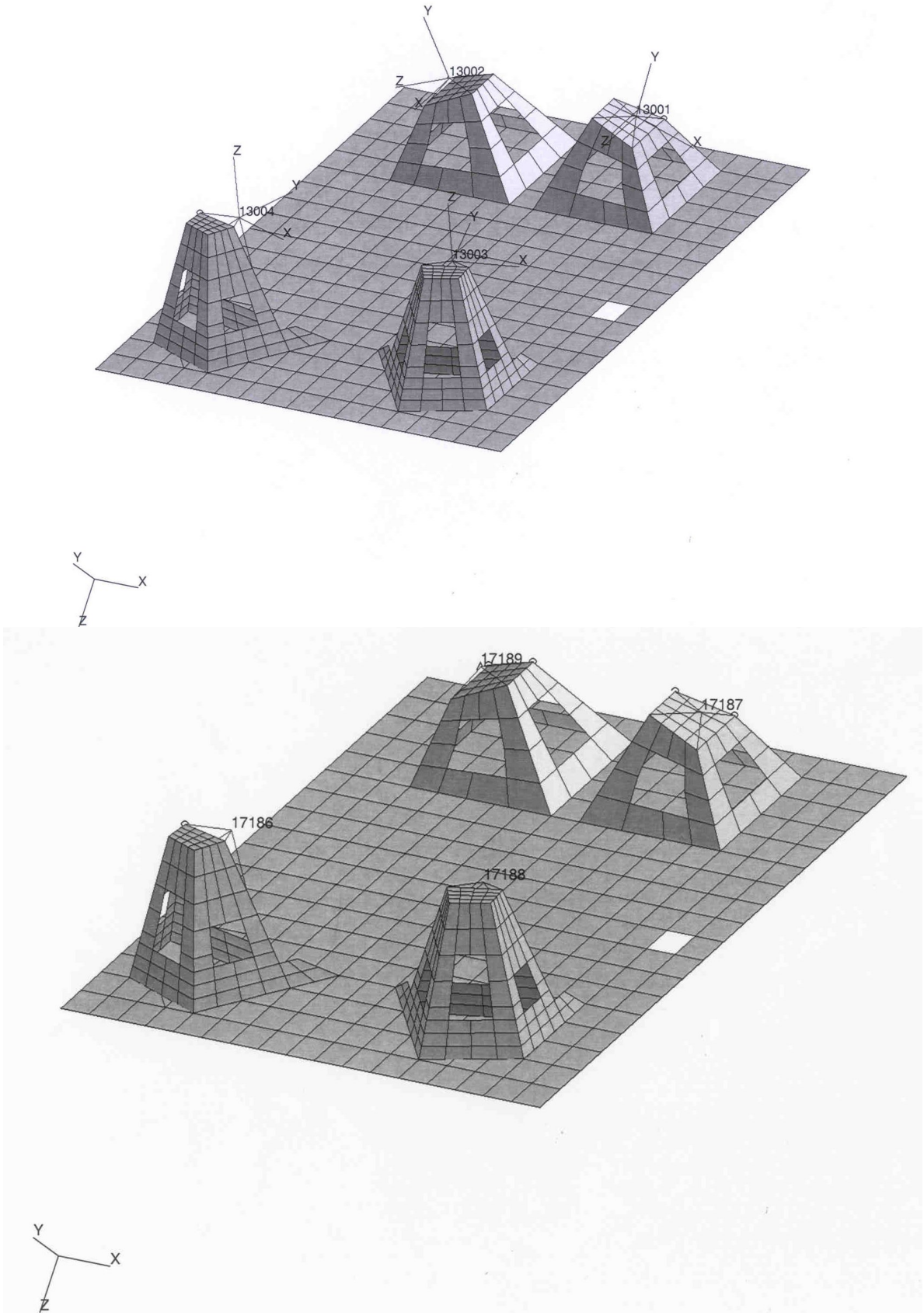

Figure 2 : Model of reaction wheels mounted on Z+/Y- panel

5 MICRO-VIBRATION ANALYSIS

5.1 NASTRAN analysis

The Nastran model used is the same as the one from sine analysis described in ref. [2]. Therefore the model is representative of the Herschel dynamic behaviour up to 140 Hz. Results at higher frequencies must be considered with caution. Nevertheless the main contribution to the Spire optical instrument, which dynamical behaviour is taken into account in the model with as spring-mass system, occurs below 120 Hz (see figure 7; maximum responses due to 16.4*6 ≈ 98.3 Hz; 19.6*5≈ 98.3 Hz; 24.56*4= 98.3 Hz; 32.8 *3≈ 98.3 Hz)

The only differences between the sine model and the one used here are the damping factor (0.005), the boundary conditions that are now free-free. The modal analysis is performed between 0 and 300Hz and the modes are normalised to the generalised mass of the Herschel S/C.
The output of the analysis includes the modal displacement, for each mode, at the SPIRE FPU as well as at the nodes representing the reaction wheels.

5.2 MICROVISION analysis

The data required to perform the microvibration analysis are the following:

- A Nastran punch file containing the modes (up to 300Hz) as well as modal displacements at the reaction wheels and at the Spire instrument location.
- Modal damping is set to 0.005.
- Characteristics of the wheels:
  - Rotating speed of the wheel: 0 to 45Hz.
  - Static Imbalance: 2 e^{-5} kg.m for the first harmonic (guaranteed by TELDIX) The relative contribution of the harmonics is extracted from the ref. [4]. Nine harmonics are taken into account for each excitation-axis. The harmonic 0.59 has been taken into account, it is typical of bearing cage excitation. According to previous studies, its amplitude is set to 2.487 e^{-6} kg.m.

	Radial excitation	Axial excitation
Harmonic number	Static imbalance (kg,m)	Static imbalance (kg,m)
0,59	2,487E-06	2,487E-06
1	2,000E-05	2,000E-05
2	3,420E-07	4,559E-07
3	3,206E-07	4,328E-07
4	3,180E-07	4,266E-07
5	3,161E-07	4,187E-07
6	3,103E-07	4,116E-07
7	3,078E-07	4,104E-07
8	3,040E-07	4,053E-07
9	2,337E-07	2,922E-07

Table 2

Excitation force input : see appendix 1

- The axial excitation are not totally negligible (see measured curve annex A). In conservative way, the radial static imbalance is considered for the 0.59 and 1 harmonic.
- The first analysis is conducted wheel by wheel, for frequencies from 0 to 300 Hz and for wheel velocity varying from 0 to 45Hz. Results provided below are the quadratic sum of the contribution of all harmonics whose frequency is below 300Hz.
- The second analysis is conducted with the four wheels rotating at the same time following the profile given in ref. [3]. Result provided below is a time-acceleration representing the accelerations of the SPIRE CoG during a 5000 seconds phase.
- Outputs are provided at node 48301, CoG of the SPIRE instrument. No specification was provided, therefore results are given in the spacecraft coordinate system.

6 RESULTS

All results are expressed in the Spacecraft coordinate system.

6.1 Contribution of each Reaction Wheel separately

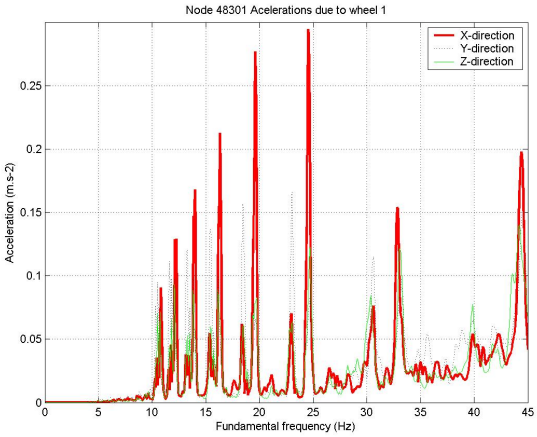

Figure 3 : RESPONSE AT NODE 48301 DUE TO REACTION WHEEL 1 (node 17188)

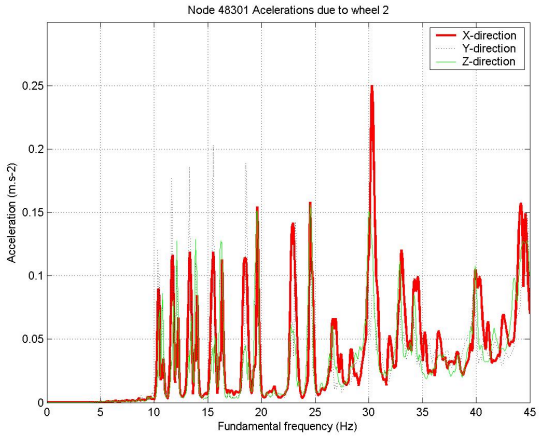

Figure 4 : RESPONSE AT NODE 48301 DUE REACTION WHEEL 2 (node 17189)

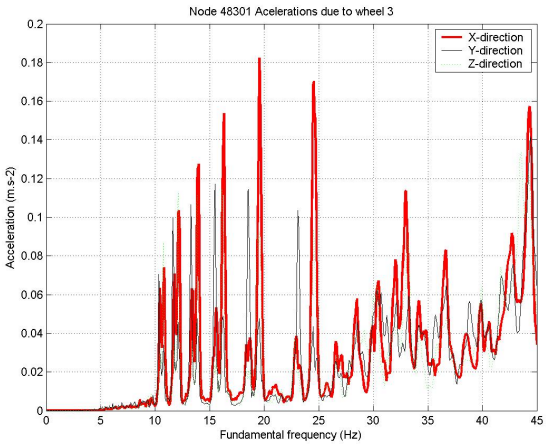

Figure 5 : RESPONSE AT NODE 48301 DUE TO REACTION WHEEL 3 (node 17186)

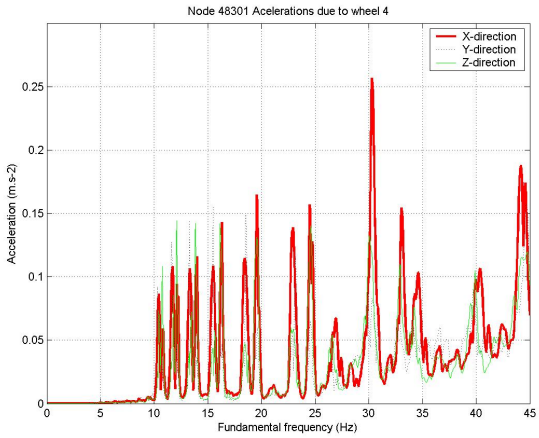

Figure 6 : RESPONSE AT NODE 48301 DUE TO REACTION WHEEL 4 (node 17187)

In this section the contribution of each wheel to the response at the SPIRE optical instrument is computed and presented in Figures 3 to 6.
The maximum acceleration is as follows:

- Due to Reaction Wheel 1: Maximum acceleration occurs at 24.6 Hz with an amplitude of 29 mg in the X direction (see Figure 3).
- Due to Reaction Wheel 2: Maximum acceleration occurs at 30.3 Hz with an amplitude of 25 mg in the X direction (see Figure 4).
- Due to Reaction Wheel 3: Maximum acceleration occurs at 24.6 Hz with an amplitude of 18.3 mg in the X direction (see Figure 5).
- Due to Reaction Wheel 4: Maximum acceleration occurs at 30.3 Hz with an amplitude of 26 mg in the X direction (see Figure 6).

With the PDR Wheel profile, the SPIRE acceleration are similar (15 mg). The difference is due to the new wheel profile (see appendix 1, with the wheel dynamic behaviour).

6.2 Sensitivity on the damping factor

The objective of this section is to investigate the impact of the cryo-temperature conditions of the HPLM on the results.

Figure 7 here below shows the contribution of each harmonic due to wheel 3 in X-direction :

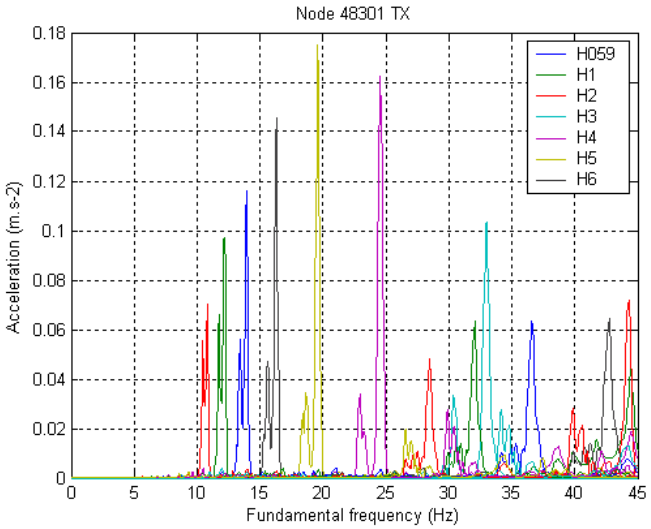

Figure 7

It shows that response at 19.6 Hz and at 24.5 Hz are respectively due to the 5th and the 4th harmonic.
It corresponds to the same mode at 98.3 Hz (4*24.56 ≈ 5*19.6 ≈ 98.3 Hz).
A previous strain energy analysis has shown that most of the energy of that mode comes from the CVV_FRAME (appendix 2). To estimated an eventual damping evolution at cryo temperature, the structural damping factor has been reduced to 0.05% (very unfavourable).

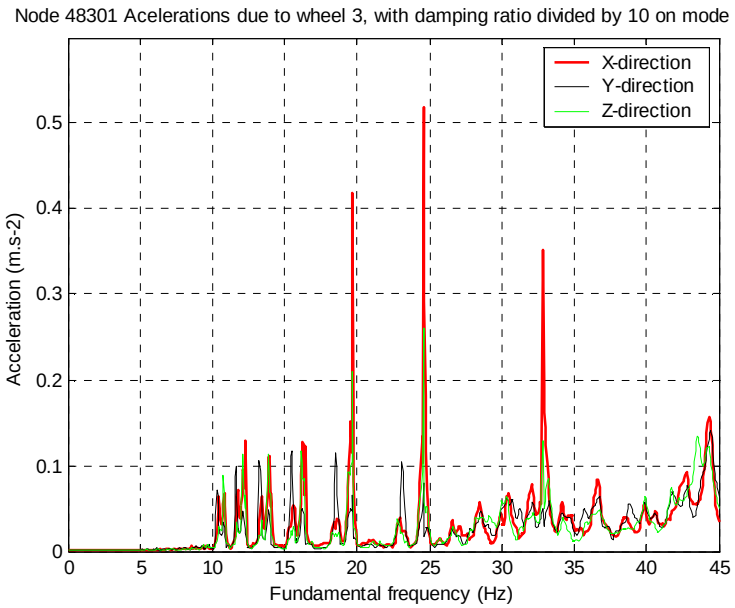

Figure 8

If we compare these curves with the curve fig 5, we can see that the two maximal amplifications have been multiplied by almost a factor 3.
It means that the choice of the damping factor values, at least for the modes which concern the coldest areas of the satellite, have to be made carefully. A damping factor of 0.0005 is considered as very conservative in cryo-conditions.
The impact of the damping factor 0.05 % is discussed in the next chapter (§6.3)

6.3 Results for the four wheels simultaneously

As no statistical analysis has been conducted between each wheel, they are considered in phase.
In this case, each wheel speed corresponds to the profile given below (cf. ref. [3]) :

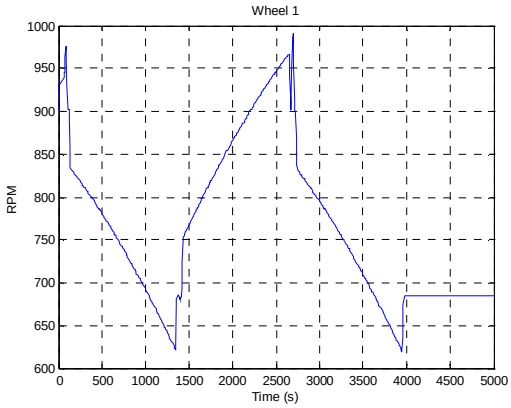

Figure 9 : SPEED PROFILE WHEEL 1 (node 17188)

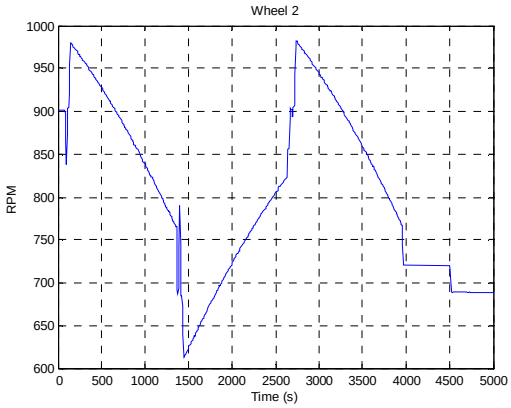

Figure 10 : SPEED PROFILE WHEEL 2 (node 17189)

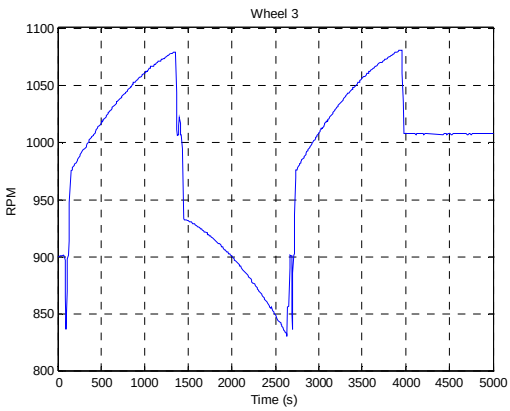

Figure 11 : SPEED PROFILE WHEEL 3 (node 17186)

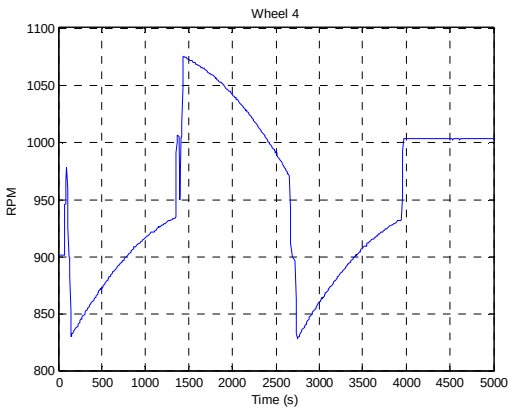

Figure 12 : SPEED PROFILE WHEEL 4 (node 17187)

Result:

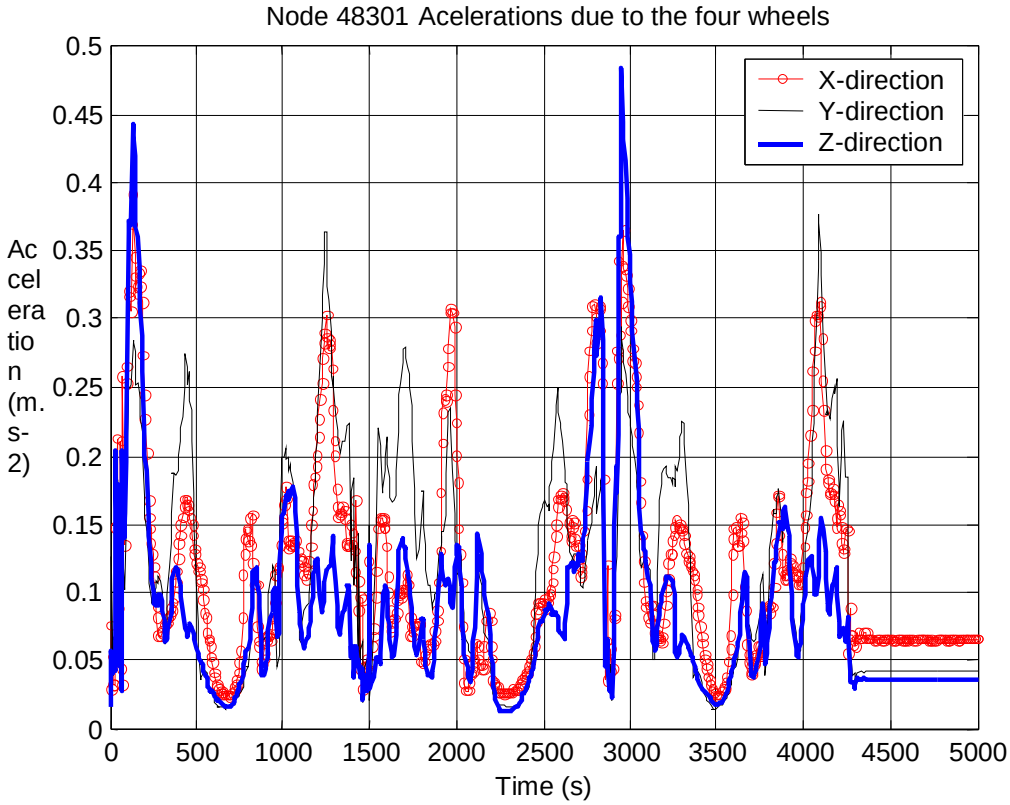

Figure 13

The maximal acceleration occurs after 125 s and has an amplitude of 39 mg in X-axis direction.
The maximal acceleration occurs after 4087 s and has an amplitude of 37 mg in Y-axis direction.
The maximal acceleration occurs after 2950 s and has an amplitude of 48 mg in Z-axis direction.

Impact with an unfavourable damping factor 0.05 %

The factor 3 (see §6.2) is at 19.6Hz/24.5 Hz (wheel speed) and the maximal wheel speed is at 1080 rpm/60= 18 Hz (wheel 3, figure 11). So, this frequency should not be excited.
However, these frequencies are close. Unfavourably, taking into account this factor 3 at 1360 s. / 3950 s. (wheel 3) and 1450 s. (wheel 4), the SPIRE maximal responses are 22*3/2= 33 mg (Y direction, at 1360/1450 s. with unfavourably 2 wheels at the same time) and 12*3=36 mg (X and Y directions at 3950 s. with unfavourably 4 wheels at the same time). (See figure 13).
These responses are covered by the maximal ones calculated with a damping factor of 0.005 (figure 13).

7 CONCLUSIONS

The Maximum acceleration obtained with one reaction wheel is 29 mg (wheel 1 excitation) at a rotating speed of 24.6 Hz in Spacecraft direction. This acceleration is mainly due to the radial wheel excitation (28 mg). Wheels 2 and 4 give almost the same level.
Acceleration levels obtained with the four wheels together following the given profile leads to a maximal acceleration level of 48 mg in Z-axis direction after 2900s.

APPENDIX 1 : EXCITATION FORCE INPUT

Radial excitation: (249 Hz:12.9 N; 241 Hz:5.7N; 264 Hz:4.4N; 234 Hz:3.2 N; 107Hz:1N; 83Hz:0.2 N; 33 Hz:0.23 N)

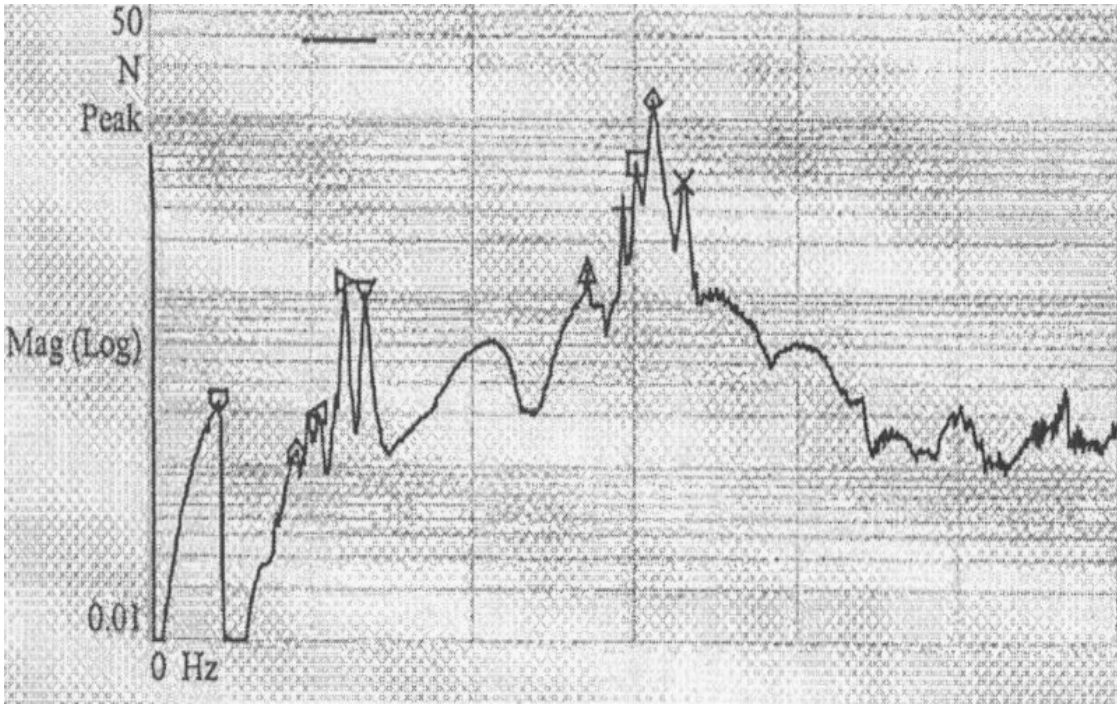

Figure 14 : Radial excitation force given by TELDIX

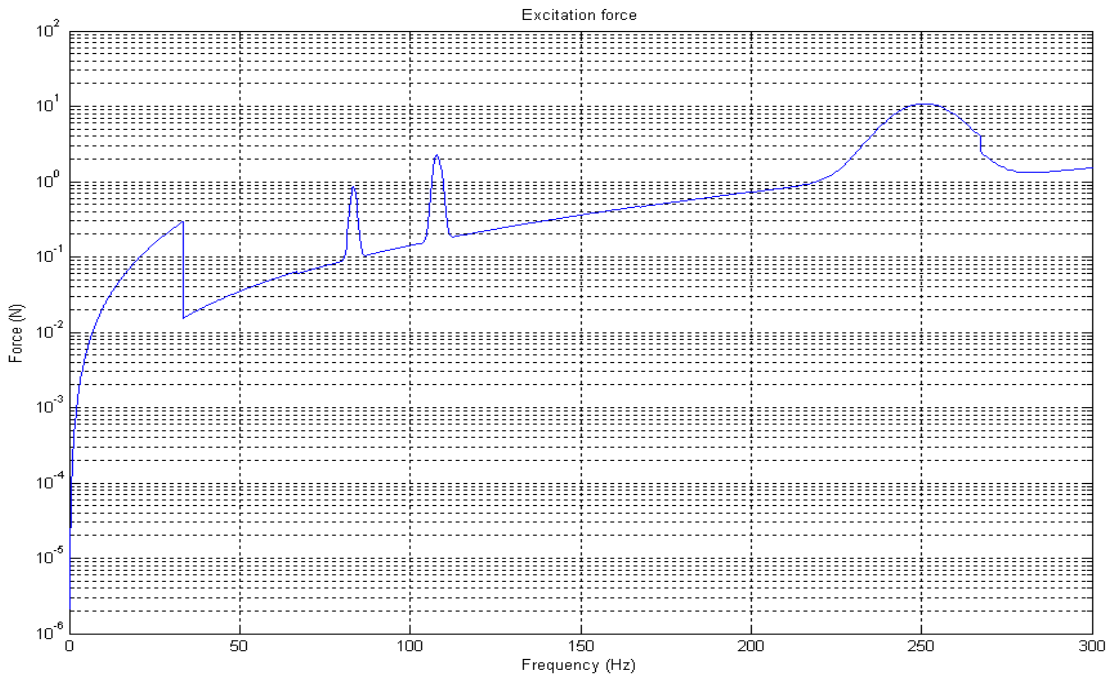

Figure 15 : Radial excitation force input

Axial excitation: (240 Hz:56 N; 234 Hz:18 N; 50Hz:0.056N)

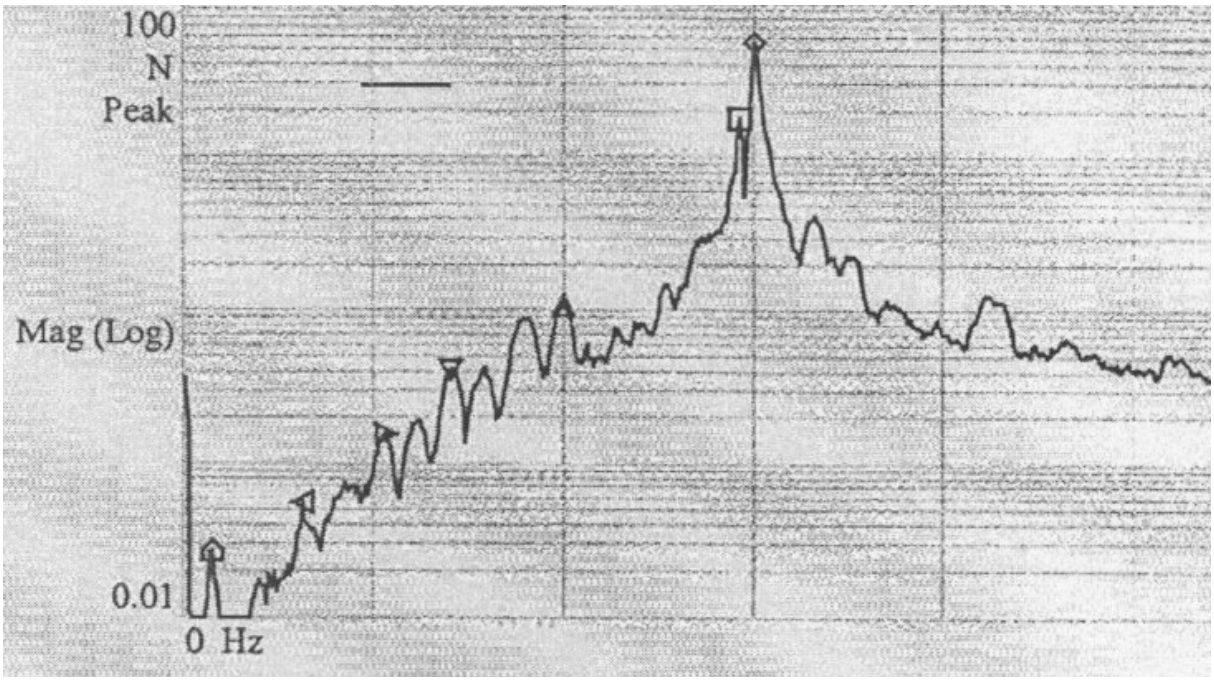

Figure 16 : Axial excitation force given by TELDIX

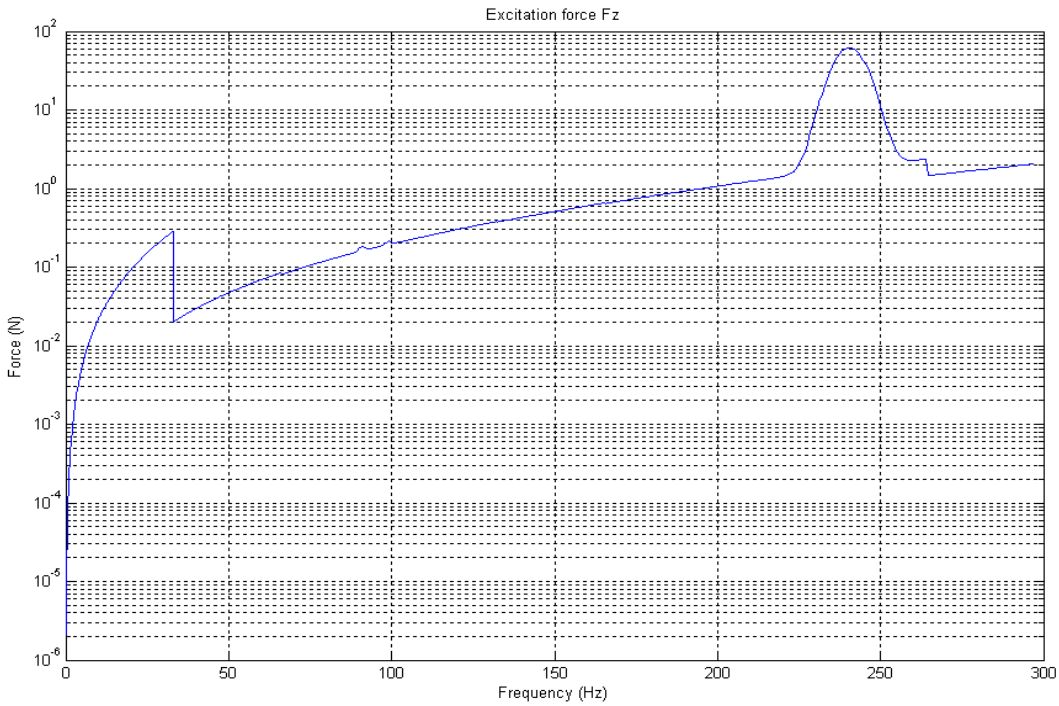

Figure 17 : Axial excitation force input

APPENDIX 2 : STRAIN ENERGY AROUND 98 HZ

MODE = 182 - FREQUENCY = 98.051 Hz

EFFECTIVE MASS & INERTIA (KG, KG.M2) :

MX	MY	MZ	IX	IY	IZ
0.000	0.000	0.000	0.000	0.000	0.000

SUBSTRUCTURE OR SUBSYSTEM	% SE	SUM
ENDEF_SVM_LOW_PLATE	63.340	63.340
ENDEF_SVM_CONE	9.398	72.738
ENDEF_SVM_OCT_Y-Z-	4.218	76.956
ENDEF_SVM_UP_PLATE	3.252	80.208
ENDEF_CVV_FRAME	2.878	83.086
ENDEF_SVM_WEB	2.639	85.724
HSS	1.800	87.524
ENDEF_HTT	1.767	89.292
ENDEF_SVM_OCT_Y-	1.264	90.555
ENDEF_OBA	1.086	91.641

MODE = 183 - FREQUENCY = 98.109 Hz

EFFECTIVE MASS & INERTIA (KG, KG.M2) :

MX	MY	MZ	IX	IY	IZ
0.000	0.000	0.000	0.000	0.000	0.000

SUBSTRUCTURE OR SUBSYSTEM	% SE	SUM
ENDEF_SVM_LOW_PLATE	28.140	28.140
ENDEF_CVV_FRAME	15.274	43.414
ENDEF_HTT	8.840	52.254
ENDEF_SVM_UP_PLATE	5.467	57.721
ENDEF_OBA	5.000	62.722
ENDEF_SVM_CONE	4.730	67.452
HSS	4.579	72.031
ENDEF_SVM_WEB	3.592	75.623
TEL	2.730	78.353
ENDEF_TEL_SUPPORT	2.685	81.038
ENDEF_SVM_OCT_Y-	2.149	83.187
ENDEF_THERMAL_SHIELD	2.076	85.264
ENDEF_CVV_PAROIS	2.059	87.323
ENDEF_SVM_OCT_Y-Z-	1.786	89.109
ENDEF_SVM_OCT_Y+	1.738	90.847
ENDEF_SVM_OCT_Y+Z-	1.067	91.914
ENDEF_SVM_OCT_Z-	1.043	92.957

MODE = 184 - FREQUENCY = 98.429 Hz

EFFECTIVE MASS & INERTIA (KG, KG.M2) :

MX	MY	MZ	IX	IY	IZ
0.000	0.000	0.000	0.000	0.000	0.000

SUBSTRUCTURE OR SUBSYSTEM	% SE	SUM
ENDEF_CVV_FRAME	23.442	23.442
ENDEF_OBA	22.576	46.018
ENDEF_HTT	18.530	64.548
TEL	8.383	72.931
ENDEF_SVM_LOW_PLATE	4.175	77.105
ENDEF_TEL_SUPPORT	3.570	80.676
ENDEF_CVV_PAROIS	2.111	82.786
ENDEF_SVM_UP_PLATE	1.766	84.553
ENDEF_SVM_WEB	1.460	86.013
HSS	1.355	87.368
ENDEF_SVM_OCT_Y+Z-	1.196	88.564
ENDEF_SVM_OCT_Y+	1.066	89.630

MODE = 185 - FREQUENCY = 98.700 Hz

EFFECTIVE MASS & INERTIA (KG, KG.M2) :

MX	MY	MZ	IX	IY	IZ
0.000	0.000	0.000	0.000	0.000	0.000

SUBSTRUCTURE OR SUBSYSTEM	% SE	SUM
ENDEF_SVM_LOW_PLATE	35.275	35.275
ENDEF_SVM_OCT_Y-Z-	21.725	57.001
ENDEF_SVM_UP_PLATE	7.847	64.848
ENDEF_SVM_OCT_Y+Z-	5.363	70.211
ENDEF_SVM_OCT_Z-	3.864	74.075
TEL	2.886	76.961
HSS	2.522	79.483
ENDEF_SVM_CONE	2.405	81.888
ENDEF_SVM_OCT_Y+	2.094	83.982
ENDEF_THERMAL_SHIELD	1.949	85.931

ENDEF_HTT	1.725	87.657
ENDEF_CVV_FRAME	1.661	89.318
ENDEF_SVM_WEB	1.278	90.596
ENDEF_OBA	1.055	91.650

END OF DOCUMENT